Nanoscale

Accepted Manuscript

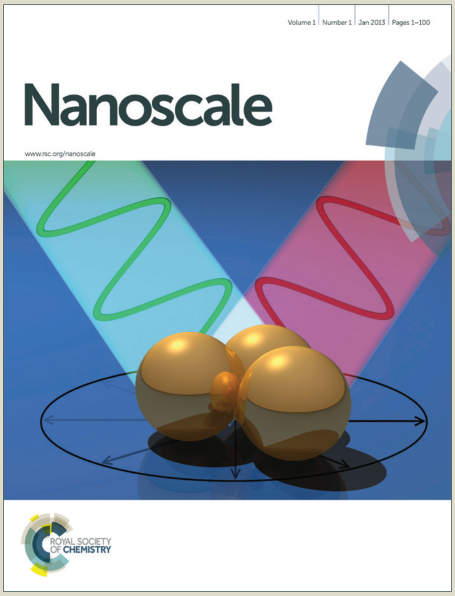

ROYAL SOCIETY OF CHEMISTRY

www.rsc.org/nanoscale

Measuring Graphene Adhesion using Atomic Force Microscopy with a Microsphere Tip

Tao Jiang[a,b] and Yong Zhu[a,*]

[a]Department of Mechanical and Aerospace Engineering, North Carolina State University, Raleigh, North Carolina 27695, USA
[*]E-mail: yong_zhu@ncsu.edu

[b]Present address: Department of Aerospace and Mechanical Engineering, University of Notre Dame, Notre Dame, Indiana 46556, USA

Keywords: adhesion energy, atomic force microscope, van der Waals force, Maugis-Dugdale theory, surface roughness

Abstract

Van der Waals adhesion between graphene and various substrates has an important impact on the physical properties, device applications and nanomanufacturing processes of graphene. Here we report a general, high-throughput and reliable method that can measure adhesion energies between ultraflat graphene and a broad range of materials using atomic force microscopy with a microsphere tip. In our experiments, only van der Waals force between the tip and a graphene flake is measured. The Maugis-Dugdale theory is employed to calculate the adhesion energy. The ultraflatness of monolayer graphene on mica eliminates the effect of graphene surface roughness on the adhesion, while roughness of the microsphere tip is addressed by the modified Rumpf model. Adhesion energies of monolayer graphene to SiO_2 and Cu are obtained as 0.46 and 0.75 Jm^{-2}, respectively. This work provides valuable insight into the mechanism of graphene adhesion and can guide the adhesion measurement for other 2D nanomaterials.

1. Introduction

The two-dimensional carbon allotrope graphene has attracted significant interest due to its remarkable physical properties.[1,2] Interfacial properties between graphene and the supporting substrate are of great importance for many applications of graphene such as nanoelectromechanical systems,[3] stretchable electronics and nanocomposites,[4-6] as well as for nanomanufacturing processes of graphene-based devices such as transfer printing.[7] Measuring and understanding the nature of adhesion energy between graphene and different substrates is critical for both fundamental research and practical applications of graphene. Recently a few experimental studies of the graphene adhesion have been reported.[8–13] A blister test method has been used to measure graphene adhesion to SiO_2/Si substrate; the blister was formed by a nanoparticle underneath,[8] air pressure[9] or water pressure.[10] A double cantilever beam (DCB) method has been used to measure graphene adhesion to metal substrate.[11] While these experimental studies have significantly advanced understanding of graphene adhesion, large discrepancy in the measurement results has been reported.[12] In addition, these methods generally depend on specific sample fabrication processes and can not explicitly take into account surface roughness. Therefore, a general, easy-handling and high-throughput method that can reliably measure adhesion between graphene and a variety of materials is in great need.

Atomic Force Microscopy (AFM) has become a well-established method for nanotribology studies including adhesion measurement.[14–16] AFM enables both high-resolution imaging of the surface and accurate measurement of interface forces and displacements. To convert the adhesion force measured by AFM to adhesion energy, a continuum mechanics model is needed. A number of such models have been developed including the well-known Johnson- Kendall-Roberts (JKR) model[17] and Derjaguin-Muller-Toporov (DMT) model,[18] which consider the interaction of an ideal sphere with an atomically flat surface. Due to the fact that the size and shape of a conventional AFM probe tip is challenging to measure and its shape is typically not spherical, a microsphere probe tip that can be attached to a tipless AFM cantilever has been used in the adhesion study.[19,20]

In this paper we present a new method to measure adhesion between graphene and different materials using AFM with a microsphere tip. The adhesion force between graphene and the spherical tip is measured by AFM using the force spectroscopy mode, and then the adhesion energy can be calculated using the Maugis-Dugdale model.[21] In our experiment, a graphene flake is placed on top of an atomically flat mica substrate, which eliminates the effect of graphene surface roughness on the adhesion, while the effect of surface roughness of the spherical tip is addressed by the modified Rumpf model.[22,23] Adhesion measurements can be performed on a large number of locations on the same graphene sample using the adhesion mapping technique. To demonstrate the utility of this method, as-received SiO_2 tips and tips coated with Cu were used to measure adhesion energies of monolayer graphene to SiO_2 and Cu, respectively, with the values of 0.46 and 0.75 Jm^{-2}.

2. Results and Discussion

In ambient condition the adhesion force typically consists of van der Waals force, capillary force and electrostatic force.[24] The capillary force is due to the presence of a condensed meniscus of water on the sample and tip surfaces. To remove the capillary force, pure nitrogen gas was flown into the AFM (Park System XE-70) chamber through a small opening. The Relative Humidity (RH) inside the chamber was monitored. The adhesion force, which is the AFM pull-off force in our experiment, was measured as a function of the RH, as shown in Fig. 1. The force was found to decrease as RH dropped owing to the decreasing capillary force, as expected.[25,26] Of particular interest is that when RH was below 23%, the adhesion force remained constant, indicating that the capillary force was eliminated. During all the adhesion measurements reported here, RH inside the AFM chamber was kept at about 0.3% to ensure no presence of the capillary force. In addition, a static eliminator (Staticmaster

Ionizer, Fischer Scientific) was placed inside the AFM chamber, facing the AFM tip and graphene sample at a distance of a few centimeters to neutralize any charges on the AFM tip and sample and thus to eliminate the electrostatic force.[27]

Monolayer graphene samples were deposited on a mica substrate by mechanical exfoliation.[28] Surface roughness of monolayer graphene samples on mica and the bare mica substrate was measured using the non-contact mode of AFM. The roughness was measured over an area of 40 × 40 nm, comparable to the contact area during the adhesion tests.[20] Three-dimensional AFM images of mica and a monolayer graphene on mica, along with their height histograms are displayed in Fig. 2(a)-(c). The root-mean-square (RMS) roughness values of mica and monolayer graphene on mica are 45 and 42 pm, respectively. Monolayer graphene has a roughness similar to that of the substrate, indicating it conforms closely to the substrate.[29,30]

The roughness of SiO_2 and Cu spherical tips was measured by AFM too, using the reverse imaging technique.[31] That is, the AFM spherical tip scans over a calibration grating (TGT1, NT-MDT Inc.) comprising an array of sharp spikes in the contact mode, which produces an image consisting of an array of the spherical caps. This image confirms that the tip is generally smooth and spherical. After the image is flattened, the roughness can be measured (see Fig. 2(d)-(f)). The measured roughness values of SiO_2 and Cu spherical tip are 183 and 475 pm, respectively, close to their flat counterparts fabricated by the same methods. It is known that surface roughness significantly affects the measured adhesion force.[24,32,33] In this work, the adhesion energies were obtained from monolayer graphene on mica and AFM spherical tips, which automatically eliminated the effect of the substrate (graphene) roughness. The tip roughness will be taken into account later using the modified Rumpf model with the measured tip roughness.

Force – displacement curves were recorded between the spherical (SiO_2 and Cu) tips and freshly prepared graphene samples using the AFM force spectroscopy mode. Before and after the AFM measurement, the SiO_2 and Cu spherical tips were imaged in a scanning electron microscope (SEM) and by AFM using the reverse imaging technique to determine their radii of curvature and assess if they were plastically deformed and/or there were any contaminations. SEM images of the SiO_2 spherical tip after AFM measurement are shown in Fig. 3. No plastic deformation or contaminant on surfaces of the tips was found. In addition, AFM images as well as Raman spectra of graphene before and after the force measurement were measured and displayed in Fig. 4. The AFM image in Fig. 4(c) shows that the graphene flake is intact after the force measurement, showing no local damages such as cracks or delamination. This is further confirmed by the Raman spectra in Fig. 4(d) – the absence of D peak (~ 1340 cm^{-1}) in both the spectra indicates no defect existent in the graphene before and after the force measurement. The intactness of both AFM spherical tips and graphene flakes after the force measurement confirms that the measurement does not cause plastic deformation of the tip, damage in the graphene flakes or delamination between the flakes and the substrate. Thus the experiment is reliable and repeatable.

The force – displacement curve measured between the SiO_2 tip and a monolayer graphene flake on mica is shown in Fig. 4(b), in which the red curve corresponds to the trace procedure while the blue curve corresponds to the retrace. Note that in Fig. 4(b), the x-axis represents the movement of the AFM z-scanner, which includes the deflection of the AFM cantilever and is much larger than the movement of the AFM tip. The pull-in point is depicted by the sudden tension (attractive force) during trace (red curve). The adhesion (pull-off) force is acquired as the maximum tension in the retrace curve (blue curve).[34] Elimination of the capillary and electrostatic forces in the experiments ensured the measured adhesion force is van der Waals force between the spherical tip and graphene. There are two additional advantages of this method: 1) a large number of adhesion measurements can be performed on the same sample using the adhesion mapping technique (e.g., 16 measurements at the locations defined by the grid lines in Fig. 4(a)); 2) the AFM image can be used to select the locations where adhesion measurements take place, such that locations with contaminations can be avoided.

The nominal adhesion energy between two flat surfaces can be obtained from the adhesion force between a sphere and a flat surface by the Maugis-Dugdale theory (assuming both surfaces are ideal without roughness)

$$W_{adh} = \frac{F_{adh}}{\lambda \pi R_{tip}} \quad (1)$$

where W_{adh} is the adhesion energy per unit area of the two flat surfaces, F_{adh} is the adhesion force between the sphere and the flat surface, R_{tip} is the radius of the sphere, and λ is an effective coefficient in the range of $1.5 \leq \lambda \leq 2.0$. The Maugis-Dugdale model reduces to the JKR model or the DMT model in the limit of $\lambda = 1.5$ or 2.0, respectively. To choose the most appropriate model, a self-consistent program based on the Maugis-Dugdale model and experimental data[35] yielded $\lambda = 1.66$ for SiO_2 and $\lambda = 1.77$ for Cu (see Supporting Information Note S1). In our case, F_{adh} is the pull-off force in the AFM force – displacement curve measured with the spherical AFM tip (SiO_2 or Cu) on monolayer graphene deposited on mica. Using Eq. (1), nominal adhesion energies of 0.18 and 0.11 Jm^{-2} were obtained for the graphene/SiO_2 and graphene/Cu interfaces, respectively.

It is well known that the surface roughness of either or both contacting surfaces affects the measured adhesion energy. In our case, the substrate (graphene on mica) is assumed to be atomically flat, and only the tip roughness is considered. The modified Rumpf model has been shown by both experiments and simulations to be able to effectively account for the effect of the surface roughness.[23] Using the modified Rumpf model, the true adhesion energy is given by

$$W_{adh} = \left[\frac{F_{adh}}{\lambda \pi R_{tip}} \right] \frac{\left(1 + \frac{R_{tip}}{1.48 R_{atomic}}\right)^{-1} + \left(1 + \frac{1.48 R_{atomic}}{z_0}\right)^{-2}}{\left(1 + \frac{R_{tip}}{1.48 R_q}\right)^{-1} + \left(1 + \frac{1.48 R_q}{z_0}\right)^{-2}} \tag{2}$$

where z_0 is the equilibrium separation of the surfaces (0.30 nm for graphene on SiO_2[36] and 0.36 nm for graphene on Cu[37]), R_{atomic} is the roughness of atomically flat surface (~ 0.03 nm), and R_q is the tip RMS roughness.

The Maugis-Dugdale model together with the modified Rumpf model was employed to calculate the adhesion energy from the adhesion force. The adhesion energies between monolayer graphene and SiO_2 and Cu are plotted in Fig. 5. The results show that the adhesion energies for graphene/SiO_2 and graphene/Cu interfaces are 0.46 and 0.75 Jm^{-2}, respectively. As can be seen from Fig. 5, the adhesion measurements are consistent and repeatable, with a maximum fluctuation of 5% over all the measured data.

The pull-off instability of AFM should be mentioned as it might affect the accuracy of the method reported here. In general, the measured pull-off force is not always the maximum attractive force (or adhesive force) as a result of the pull-off instability. However, the pull-off force is a good measure of adhesion if the materials are fully elastic with little or no viscoelastic character, the interface is chemically stable, and the cantilever stiffness is much lower than the adhesive force gradient, which is in turn much lower than the contact stiffness.[14] In our case, the contact materials (graphene, SiO_2 and Cu) are all elastic. The adhesion is due to van der Waals force that is chemically stable. The adhesive force gradient was calculated based on the Lennard-Jones potential for the graphene/SiO_2 or graphene/Cu interface, which is much larger than the cantilever stiffness but smaller than the contact stiffness (see Supporting Information Note S2 for more details). Altogether, the pull-off force measurement in our case is an accurate and reliable method to measure the adhesion. The highly consistent data shown in Fig. 5 confirm the accuracy of our method.

Our measurement at the graphene/tip interface can give the upper and lower bounds of the adhesion values between graphene and substrate (assuming the substrate is made of the same material as the tip used in the AFM measurement). In one limiting case, graphene conforms to the substrate completely, graphene adhesion to the substrate should be equal to our value after the roughness correction (e.g., the upper bound of 0.46 Jm^{-2} for the graphene/SiO_2 interface). In the other limiting case where graphene is suspended on top of the substrate's roughness peaks, graphene adhesion to the substrate should be equal to our value without the roughness correction (e.g., the lower bound of 0.18 Jm^{-2} for the graphene/SiO_2 interface with the roughness of graphene on SiO_2 and SiO_2 tip to be 181 and 183 pm, respectively). For instance, as the monolayer graphene conforms to the SiO_2 substrate,[9] the measured adhesion energy, 0.45 Jm^{-2}, is very close to our value after the roughness correction. As the 2- to 5-layer graphene partially conforms to the SiO_2 substrate,[9] the measured adhesion energy, 0.31 Jm^{-2}, is between the upper and lower bounds. In our method, the surface roughness of both graphene and tip can be directly measured, which is not available in previous methods.

3. Conclusions

In conclusion, graphene adhesion energies to representative dielectric substrates (e.g., SiO_2) and metal substrates (e.g., Cu) were measured using AFM with a microsphere tip. Experimental conditions were controlled to ensure that the measured adhesion is exclusively due to van der Waals force, which is the fundamental interaction between graphene and SiO_2 or Cu substrate. The adhesion energies of 0.46 Jm^{-2} for the monolayer graphene/SiO_2 interface and 0.75 Jm^{-2} for the monolayer graphene/Cu interface were obtained. Accurate measurement of graphene adhesion energy is of great importance for both fundamental research and practical applications of 2D nanomaterials. This work has addressed two critical issues that present challenges for measurement of graphene adhesion using AFM – roughness of an AFM tip and pull-off instability that could occur during the tip-sample interaction. The reported experiment provides an important guidence for adhesion measurement between 2D nanomaterials and a broad range of materials.

4. Experimental Section

Monolayer graphene samples were deposited on freshly peeled mica substrates by the mechanical exfoliation method[28] right before the adhesion measurement. The as-received SiO_2 microsphere AFM tips (Novascan Technologies, Inc., Ames, IA, USA) were mounted onto an AFM (XE-70, Park Systems) for force measurement immediately after being moved from their vacuum pockets to avoid possible contaminations. For adhesion measurement between graphene and Cu, a thin layer of Cu was sputtered onto the AFM spherical tip. The sputtering parameters (e.g., current and time) were optimized to sputter a layer of Cu with a uniform thickness of tens of nanometers. The spring constants of AFM cantilevers were calibrated using Neumeister's method.[38] The monolayer graphene was characterized by the thickness measurement with AFM[39] and further confirmed *via* Raman spectroscopy (Horiba LabRAM HR).[40] AFM images of a monolayer graphene on mica and its Raman spectra before and after the force measurement are demonstrated in Fig. 4.

Force measurements were taken at room temperature under a RH of ~ 0.3%. For each selected monolayer graphene flake on mica substrate, measurements were taken at sixteen locations one by one. During the force measurement, AFM cantilever with microsphere tip initially approaches a graphene sample from a distance of micrometers at a low speed of 0.1 μm/s that can be regarded as quasistatic. While the tip moves towards the sample (procedure of trace), at one point the tip snaps to the sample due to the attractive van der Waals force. As the cantilever continues to move down, the force turns repulsive and the compression (repulsive force) increases. The cantilever stops moving downward and starts moving upward as the compression reaches the pre-set force limit. While the tip moves up (procedure of retrace), the force changes from repulsive to attractive. At the point of separation, the tip pulls off the sample abruptly and the pull-off force (adhesion force) can be acquired as the maximum tension in retrace from the AFM force – displacement curve.

Acknowledgements

This work was supported in part by the National Science Foundation (CMMI-1129817) and the EFRI program (EFRI-1240438).

Received: ((will be filled in by the editorial staff))
Revised: ((will be filled in by the editorial staff))
Published online: ((will be filled in by the editorial staff))

Notes and references

1 Novoselov, K. S., Falko, V. I., Colombo, L., Gellert, P. R., Schwab, M. G., Kim, K. A., Nature **2012**, 490, 192–200.

2 Lee, C., Wei, X., Kysar, J. W., Hone, J., Science **2008**, 321, 385–388.

3 Bunch, J. S., van, d. Z., Verbridge, S. S., Frank, I. W., Tanenbaum, D. M., Parpia, J. M., Craighead, H. G., McEuen, P. L., Science **2007**, 315, 490–493.

4 Kim, K. S., Zhao, Y., Jang, H., Lee, S. Y., Kim, J. M., Kim, K. S., Ahn, J., Kim, P., Choi, J., Hong, B. H., Nature **2009**, 457, 706–710.

5 Jiang, T., Huang, R., Zhu, Y., Adv. Funct. Mater. **2014**, 24, 396–402.

6 Guo, G. and Zhu, Y., ASME J. Appl. Mech. **2015**, 82, 031005.

7 Li, X. S., Zhu, Y. W., Cai, W. W., Borysiak, M., Han, B. Y., Chen, D., Piner, R. D., Colombo, L., Ruoff, R. S., Nano Lett. **2009**, 9, 4359–4363.

8 Zong, Z., Chen, C., Dokmeci, M. R., Wan, K., J. Appl. Phys. **2010**, 107, 026104(3pp).

9 Koenig, S. P., Boddeti, N. G., Dunn, M. L., Bunch, J. S., Nat. Nanotechnol. **2011**, 6, 543–546.

10 Cao, Z., Wang, P., Gao, W., Tao, L., Suk, J. W., Ruoff, R. S., Akinwande, D., Huang, R., Liechti, K. M., Carbon **2014**, 69, 390–400.

11 Yoon, T., Shin, W. C., Kim, T. Y., Mun, J. H., Kim, T., Cho, B. J., Nano Lett. **2012**, 12, 1448–1452.

12 Boddeti, N. G., Koenig, S. P., Long, R., Xiao, J. L., Bunch, J. S., Dunn, M. L., J. Appl.

Mech. **2013**, 80, 040909(8pp).

13 Na, S. R., Suk, J. W., Ruoff, R. S., Huang, R., Liechti, K. M., ACS Nano **2014**, 8, 11234–11242.

14 Carpick, R. W., Batteas, J., de Boer, M. P., Springer Handbook of Nanotechnology **2007**, D32, 951–979.

15 Burnham, N. A., Dominguez, D. D., Mowery, R. L., Colton, R. J., Phys. Rev. Lett. **1990**, 64, 1931–1934.

16 Butt, H., Cappella, B., Kappl, M., Surf. Sci. Rep. **2005**, 59, 1–152.

17 Johnson, K. L., Kendall, K., Roberts, A. D., P. Roy. Soc. Lond. A Mat. **1971**, 324, 301–313.

18 Derjaguin, B. V., Muller, V. M., Toporov, Y. P., Prog. Surf. Sci. **1994**, 45, 131–143.

19 Ducker, W. A., Senden, T. J., Pashley, R. M., Nature **1991**, 353, 239–241.

20 Heim, L., Blum, J., Phys. Rev. Lett. **1999**, 83, 3328–3331.

21 Maugis, D., J. Colloid Interf. Sci. **1992**, 150, 243–269.

22 Rabinovich, Y. I., J. Colloid Interf. Sci. **2000**, 232, 10–16.

23 Jacobs, T., Ryan, K., Keating, P., Grierson, D., Lefever, J., Turner, K., Harrison, J. A., Carpick, R. W., Tribol. Lett. **2013**, 50, 81–93.

24 Jones, R., Pollock, H. M., Cleaver, J. A. S., Hodges, C. S., Langmuir **2002**, 18, 8045–8055.

25 Paajanen, M., Katainen, J., Pakarinen, O. H., Foster, A. S., Lahtinen, J., J. Colloid Interf. Sci. **2006**, 304, 518–523.

26 Stukalov, O., Murray, C. A., Jacina, A., Dutcher, J. R., Rev. Sci. Instrum. **2006**, 77, 033704(6pp).

27 Ouyang, Q., Ishida, K., Okada, K., Appl. Surf. Sci. **2001**, 169, 644–648.

28 Novoselov, K. S., Jiang, D., Schedin, F., Booth, T. J., Khotkevich, V. V., Morozov, S. V., Geim, A. K., Proc. Natl. Acad. Sci. **2005**, 102, 10451–10453.

29 Ishigami, M., Chen, J. H., Cullen, W. G., Fuhrer, M. S., Williams, E. D., Nano lett. **2007**, 7, 1643–1648.

30 Cullen, W. G., Yamamoto, M., Burson, K. M., Chen, J. H., Jang, C., Li, L., Fuhrer, M. S., Williams, E. D., Phys. Rev. Lett. **2010**, 105, 215504(4pp).

31 Neto, C., Craig, V. S. J., Langmuir **2001**, 17, 2097–2099.

32 Gao, W., Huang, R., J. Phys. D: Appl. Phys. **2011**, 44, 452001(4pp).

33 DelRio, F. W., de Boer, M. P., Knapp, J. A., Reedy, E. D. Jr, Clews, P. J., Dunn, M. L., Nat. Mater. **2005**, 4, 629–634.

34 Moore, N., Houston, J., J. Adhes. Sci. Technol. **2010**, 24, 2531–2544.

35 Carpick, R., Ogletree, D., Salmeron, M., J. Colloid Interface Sci. **1999**, 211, 395–400.

36 Gao, W., Xiao, P. H., Henkelman, G., Liechti, K. M., Huang, R., J. Phys. D: Appl. Phys. **2014**, 47, 255301(6pp).

37 Vanin, M., Mortensen, J. J., Kelkkanen, A. K., Garcia-Lastra, J. M., Thygesen, K. S., Jacobsen, K. W., Phys. Rev. B **2010**, 81, 081408(4pp).

38 Clifford, C. A., Seah, M. P., Nanotechnology **2005**, 16, 1666–1680.

39 Obraztsova, E. A., Osadchy, A. V., Obraztsova, E. D., Lefrant, S., Yaminsky, I. V., Phys. Status Solidi B **2008**, 245, 2055–2059.

40 Graf, D., Molitor, F., Ensslin, K., Stampfer, C., Jungen, A., Hierold, C., Wirtz, L., Nano Lett. **2007**, 7, 238–242.

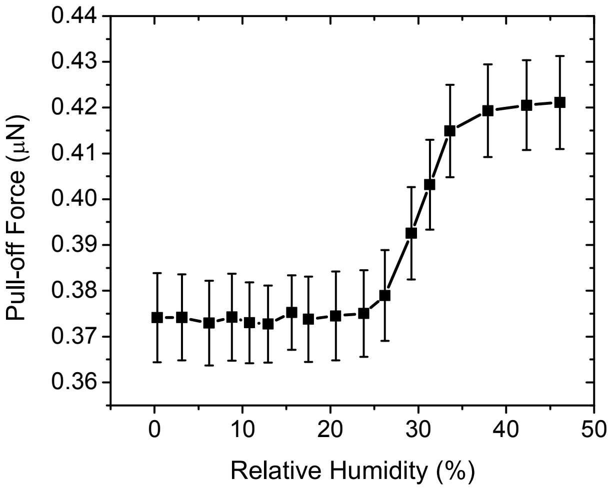

Fig. 1 AFM pull-off force for graphene on mica substrate as a function of Relative Humidity inside the AFM chamber.

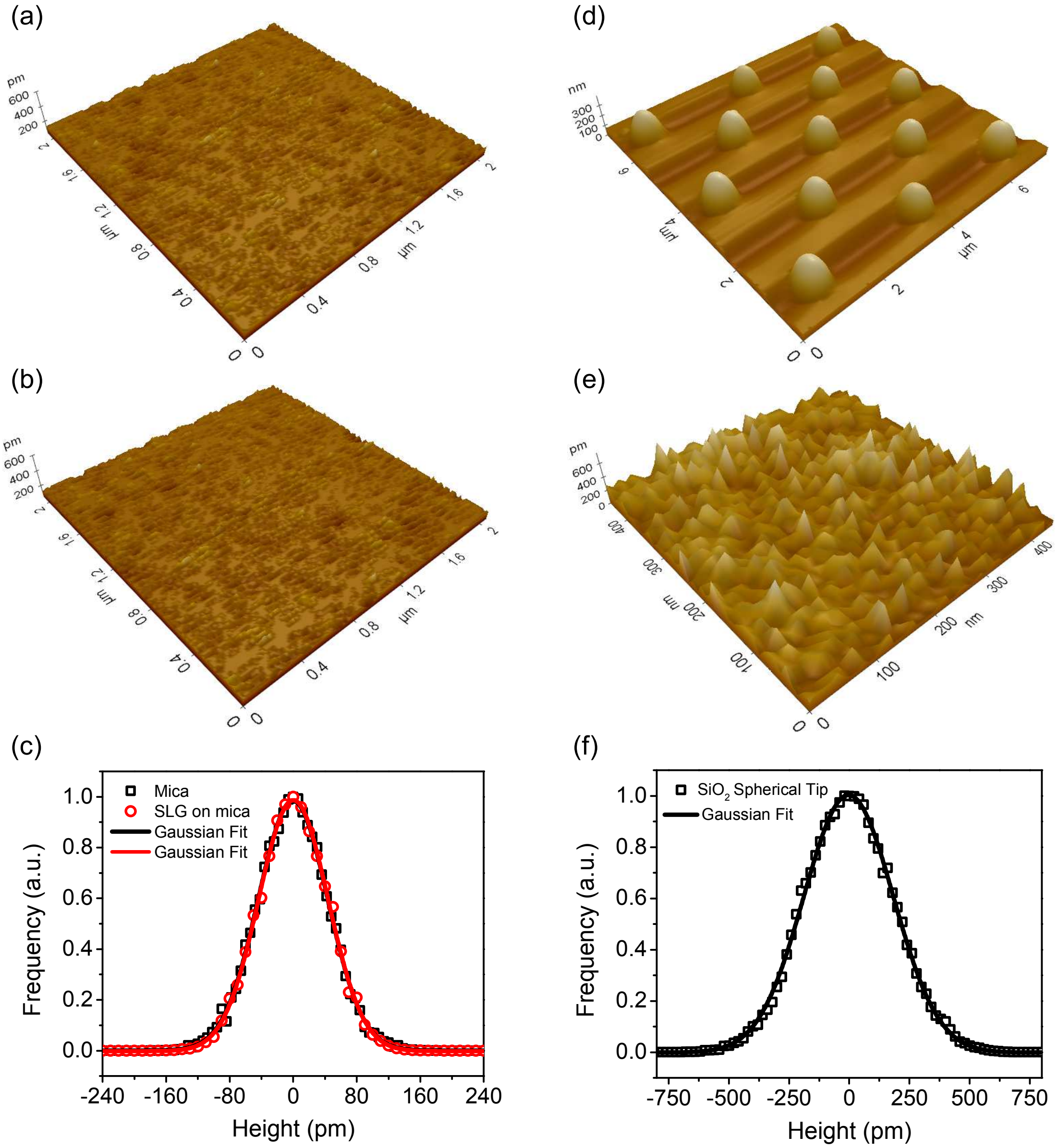

Fig. 2 3-dimensional AFM images of (a) mica and (b) single-layer graphene (SLG) on mica. (c) Height histograms for mica (black square) and SLG on mica (red circle). (d) AFM images of the SiO_2 spherical tip. Each small dome-like feature corresponds to the SiO_2 tip scanning over each spike of the AFM grating array. (e) 3-dimensional AFM image of the top area of the spherical tip after flattening. (f) Height histogram for the SiO_2 tip. In (c) and (f), height histograms are measured over an area of 40 × 40 nm, the data are fitted by Gaussian distributions with the roughness (standard deviation of distribution) to be 45, 42 and 183 pm for mica, SLG on mica and SiO_2 tip respectively.

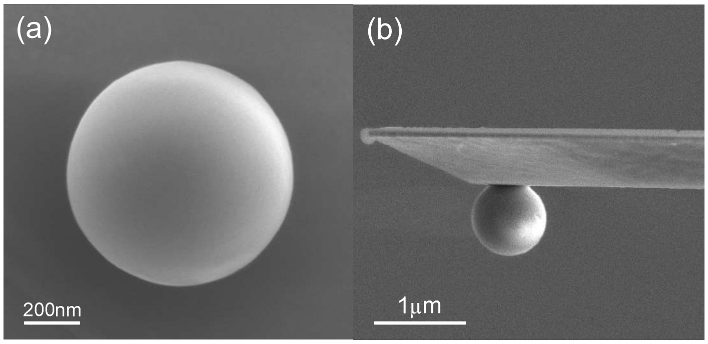

Fig. 3 SEM image of (a) AFM SiO_2 microsphere tip and (b) side view of the microsphere tip on cantilever. The images were taken after the force measurement. The radius of SiO_2 tip is 405.4 nm.

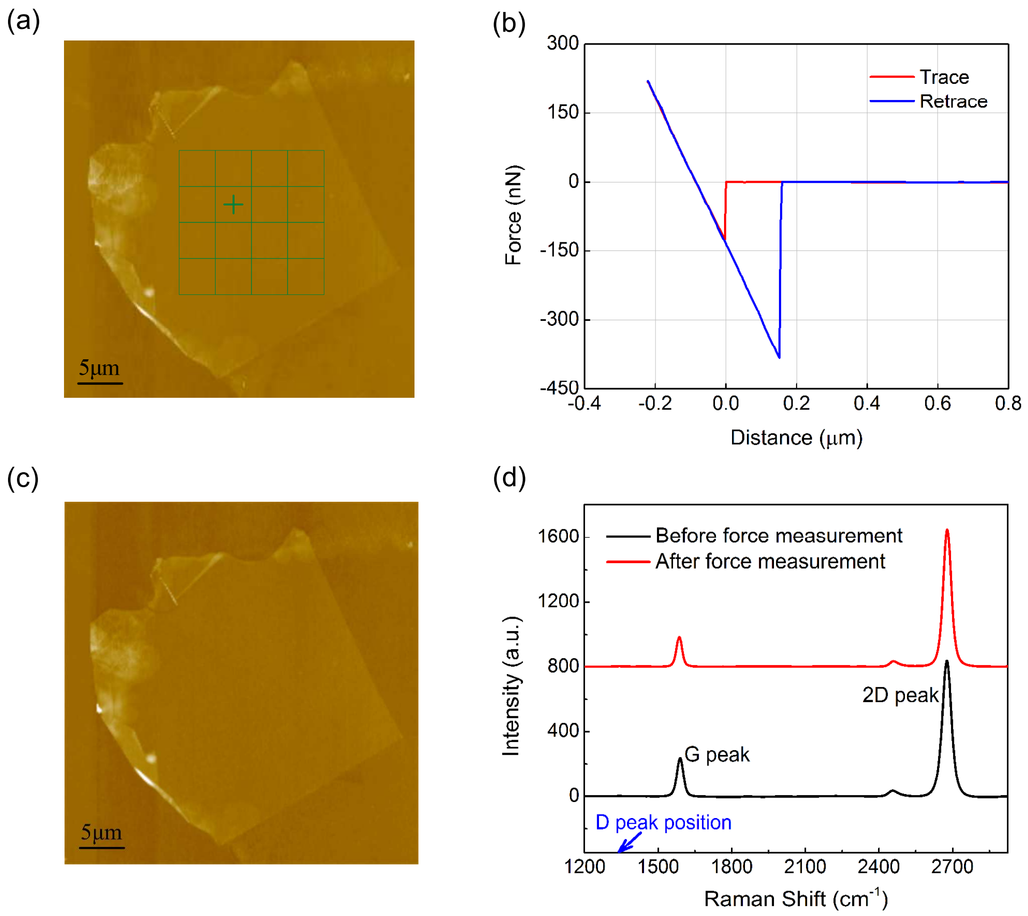

Fig. 4 (a) AFM force measurement on a mono-layer graphene flake on mica substrate. The grid on graphene's image shows 16 component blocks for the force measurement, which is taken at the center of each block (denoted by the cross). (b) Force – distance curve measured on graphene in (a) with SiO_2 spherical tip. (c) AFM image of the graphene flake in (a) after force measurement, showing no damages on the flake. (d) Raman spectra of the graphene in (a) before (black) and after (red) the force measurement. The absence of D peak (at ~ 1340 cm^{-1} position as pointed by the blue arrow) before and after force measurement indicates no damage or delamination on graphene during the measurement.

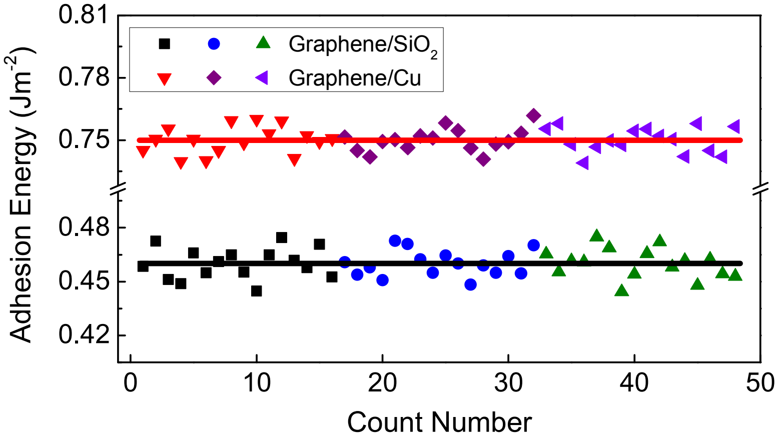

Fig. 5 Adhesion energies of graphene with SiO_2 and Cu measured using AFM spherical tips on monolayer graphene. Each dot represents the adhesion measured at one point of the mesh shown in Fig. 4(a). The symbols of the dots designate different graphene samples. The solid lines denote average adhesions of the corresponding measurements.

Measuring Graphene Adhesion using Atomic Force Microscopy with a Microsphere Tip

Tao Jiang and Yong Zhu[*]

Keyword

adhesion energy, atomic force microscope, van der Waals force, Maugis-Dugdale theory, surface roughness

Graphic Abstract

This work reports a general method to measure adhesion energies between graphene and microsphere tips made of different materials using atomic force microscopy.